Pendant Group Effect of Polymeric Dielectrics on the Performance of Organic Thin Film Transistors①

HUANG Chong-Yu[a, b, c] FENG Shi-Yu[a, b, c] HUANG Wei-Guo[a, b, c②]

[a] (*State Key Laboratory of Structural Chemistry, Fujian Institute of Research on the Structure of Matter, Chinese Academy of Sciences, Fuzhou* 350002, *China*)

[b] (*University of Chinese Academy of Sciences, Beijing* 100049, *China*)

[c] (*Fujian Science & Technology Innovation Laboratory for Optoelectronic Information of China, Fuzhou* 350002, *China*)

ABSTRACT Polymer dielectric is superior to its inorganic counterparts due to not only the low cost and intrinsic flexibility, but also the readily tunable dielectric constant, surface charge trap density, charge ejection and releasing ability and dipole moment, and all these properties play decisive roles in regulating the characteristic and performances of organic thin film transistors (OTFT). However, systematical studies on the relationship between structure and properties of polymeric dielectrics are rare. To this end, a series of polymeric dielectrics with well-defined linkages (ester or amide bonds) and predesigned pendant groups (alkyl- and aromatic-groups) are synthesized in high yields. Detailed studies show that the polyamide dielectrics exhibit higher dielectric constant, surface charge trapping density, and better charge storage capability than corresponding polyester dielectrics. Further, increasing the π electron delocalization of the pendant groups generally benefits the charge storage property and transistor memory behavior. Theoretical calculation reveals that the hydrogen bonding between the linkage groups and the energy alignment between polymeric dielectric and semiconductor are responsible for the observed performance differences of OTFT with different polymeric dielectrics. These results may shine light on the design of polymeric dielectrics for OTFTs with different applications.

Keywords: polymer dielectric, organic thin film transistor, hydrogen bonding, π-electron delocalization, noncovalent interaction; DOI: 10.14102/j.cnki.0254-5861.2011-3167

1 INTRODUCTION

Apart from semiconductors, dielectrics substantially dominate the functioning and performance of OTFTs. e.g., via affecting the charge carrier mobilities (μ), impacting the threshold voltages (Vth) and subthreshold swings (SS), determining the bias-stress instabilities and modulating the switching rate and hysteresis behaviors of OTFTs[1-6]. To date, numbers of materials have been introduced as dielectrics in OTFTs, such as inorganic oxides, organic molecules and polymers, self-assembled mono-/multilayers (SAMs) and self-assembled nanodielectrics (SANDs)[2, 7]. Among them, polymeric dielectrics are particularly interesting owing to: i) their intrinsic flexibility and stretchability are naturally compatible with the organic semiconductors and flexible substrates underneath[2, 8]; ii) the low-cost and energy-saving fabrication procedures such as drop-casting, spin-coating and role to role printing. Comparatively, the fabrication of inorganic dielectrics usually involves expensive and energy-consuming e-beam sputtering, atomic layered deposition, and high temperature evaporation[9, 10]; iii) the robust tunability of chemical structures by rational molecular design and facile organic synthesis, allowing on-demand functionalization for a variety of purposes, such as biochemical sensing, neuromorphic devices, stretchable and self-healable electronics and biodegradable devices. Moreover, such capability enables the possibility to investigate the comprehensive mechanisms of device physics via subtle structure tailoring[3, 11].

Received 2 March 2021; accepted 13 April 2121

① This work was supported by the start-up funding from FJIRSM-CAS, and National Natural Science foundation of China (51803214). W.G.H is also grateful for the award of "The Recruitment Program of Global Youth Experts"

② Corresponding author. E-mail: whuang@fjirsm.ac.cn

Despite this promise, polymer dielectrics generally complicate their behaviors and performances by their less-ordered structures, broad molecular weight (MW) distributions and glass transition temperatures (T_g), uncertain chain alignments and dipole orientations, varied crystallinity and packing mode, etc[8]. For example, increasing dielectric constant (κ) of polymer leads to higher capacitance (C), though at the price of broadening density of state (DOS) and disordering the dipoles, which eventually impedes the transfer of charge and affects mobilities[1, 12, 13]. Interestingly, upon increasing κ of polymer dielectrics, polymeric semiconductor exhibits enhanced mobility whereas single-crystalline semiconductor decreases its mobility[14]. The effect of molecular weight to the performance of OTFTs is also under debate. Some studies suggest that varying the molecular weight could cause mobility change up to 2 orders of magnitude, probably attributing to the alternation of polymer chain ends density on the dielectric surface and thus the interfacial energy[15, 16]. However, other reports pointed out that molecular weight only leads to subtle changes to the major characteristics of OTFTs[17]. In addition, the surface properties of polymeric dielectric impose further complexity to OTFT performances. e.g., some reports indicated that lowering the surface energy leads to smaller grain size of semiconductor and more interconnections between grains and therefore enhances the charge transfer[18, 19]. Conversely, other studies made completely opposite claims[15]. The controversy may be arisen from different semiconductors and fabrication approaches used in the experiments, as well as the complicacy of the interplay among grain size, boundaries and charge mobilities. Up to now, it is still a great challenge to unambiguously clarify the influence of a given variable to the OTFT performances while excluding all other factors. And systematical studies on the relationship between structure and properties of polymeric dielectrics are rare.

To this end, here we have designed and synthesized a series of well-defined polymeric dielectrics bearing pendant groups with progressively enhanced π electron delocalization. These pendant groups are linked with polymer backbones via ester or amide bonds. Note that all these polymers gain similar molecular weight and MW distributions, so as to eliminate the effect from chain ends density and heterogeneity on the dielectric surfaces. Detailed studies reveal that the polyamide dielectrics exhibit higher κ and surface charge trapping density, and better charge storage capability than the corresponding polyester dielectrics. Moreover, as the π electron delocalization increases, the energy barrier between the nearest molecular orbital levels of semiconductor (such as the highest occupied molecular orbital (HOMO) and the lowest unoccupied molecular orbital (LUMO)) and the polymeric dielectric reduces, which facilitates the charge transfer from conductive channel to dielectric layer upon biasing with gate voltages[20]. As a result, the OTFT exhibits more pronounced bias-stress instability and larger hysteresis. Theoretical calculation indicates that the hydrogen bonding between the amide groups and the energy alignment between polymeric dielectrics and semiconductor are responsible for the observed distinctness of OTFTs with different polymeric dielectrics. These results may help to gain a clearer understanding of the relationship between structures and properties of polymeric dielectrics, and shine light on the design of polymeric dielectrics for OTFTs with different applications.

2 COMPUTATIONAL DETAILS

Theoretical calculations of one monomer and two repeated units of the polymer were carried out, respectively. Geometry optimizations and frequency analyses were implemented by ORCA 4.2.1 program using dispersion corrected methods B3LYP-D3 (B3LYP with Grimme's DFT-D3 correction) in conjunction with the def2-TZVP basis set[31].

3 RESULTS AND DISCUSSION

3. 1 Synthesis and characterization of polymeric dielectrics

Acrylate and acrylamide monomers were synthesized by reacting acryl chloride with corresponding alcohols and alkylamines, respectively (Fig. 1a). Subsequent polymerizing the monomers by reversible addition fragmentation chain transfer (RAFT) reaction in 1,4-dioxane gives polymers as white solids in good yields (> 80%), requiring only precipitation and centrifugation for purification. In the following text, poly(octyl acrylate), poly(benzyl acrylate) and poly(naphthalen-1-ylmethyl acrylate) are denoted as A1, A2 and A3, respectively, and poly(N-octyl acryamide), poly(N-benzyl acrylamide) and poly(N-(naphthalen-1-ylmethyl)-acrylamide) are named as B1, B2 and B3, respectively (Fig. 1b). 1H NMR spectra unambiguously confirm their chemical structures (Fig. S1). Gel permeation chromatography (GPC) characterizations show that all these polymers

gain molecular weight ranging from 12,000 to 24,000 with narrow polydispersity index (1.3~1.6, Table S1). Thermogravimetric analysis (TGA) and differential scanning calorimetry (DSC) tests indicate that the thermal stability and glass transition temperature (T_g) increase with the rigidity of the pendant group (Fig. S2, S3), in good agreement with previous reports[21]. Water contact angle tests (Fig. S4) reveal that the polyamides (B1, B2 and B3) exhibit higher hydrophilicity than the corresponding polyesters (A1, A2 and A3).

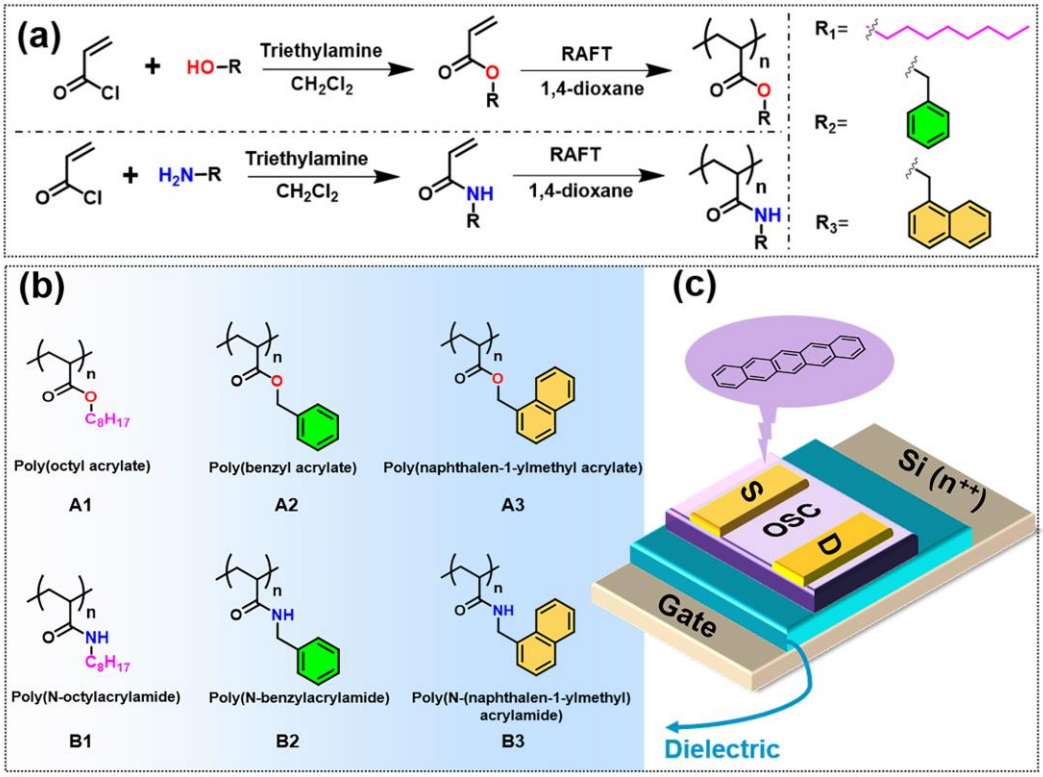

Fig. 1. (a-b) Synthesis route and chemical structures of polymer dielectrics. (c) Device architecture of organic thin film transistor

3. 2 Device fabrication and characterizations

Device fabrication and characterizations dielectric capacitance and leakage current density of the polymers are investigated by using devices with MIM configuration (metal-insulator-metal). The thickness of the films is around 1000 nm. As shown in Fig. 2a and Fig. S5, these polymer dielectric films show typical frequency-dependent capacitance spanning from 35 to 111 nF/cm^2 (κ: 2.1~6.5 @20 Hz). Moreover, the capacitance of polyamide is ~2 times larger than the value of polyester counterparts. Varying the pendant groups gives rise to negligible influence to the capacitance. To explain the higher capacitance of polyamides than polyesters, a hypothesis suggests the amide group serves as a localized molecular dipole pointing from the oxygen to nitrogen atom. In the absence of external electric field, these dipoles are randomly orientated. However, upon applying an external electric field, these dipoles realign themselves and form apparent large dipoles across the film (Fig. 2b). The resulting large dipole moment enables more induced charge carriers and therefore enhances the capacitance. Moreover, the hydrogen bonds between neighboring amide groups further strengthen the alignment and slow down the dipole relaxation, leading to more pronounced hysteresis behavior (*vide infra*). In contrast, the dipole moment of ester group (2.2~2.6 D) is much smaller than the value of amide group (3.8~4.0 D), resulting in weak interaction between the external electric field and ester groups and reducing the capacitances. Additionally, the absence of hydrogen bonding between ester groups helps to dissociate the alignment rapidly and gives rise to good bias-stress stability (*vide infra*).

It's well-known that noncovalent interaction plays an important role in spatial arrangement of molecules[22, 23], so noncovalent interaction (NCl) analysis for these six polymers is conducted based on a model developed by Yang[24-26]. In this model, the quantum-mechanical electron density, ρ, and the reduced density gradient, s ($s = 1/(2(3\pi^2)^{1/3})|\nabla\rho|/\rho^{4/3}$), are the two fundamental quantities for describing the deviation from a homogeneous electron distribution. Covalent

bonding and noncovalent bonding could be well distinguished from the plot of s versus ρ. In detail, plot pattern of covalent bond shows small electron density and large reduced gradient corresponding to the exponentially decaying tail regions (far from the nuclei) of the electron density, and large electron density and low reduced gradient corresponding to the covalent bond. A saddle point in the electron density (bond critical points, s = 0) is the characteristic of covalent bonds, whereas noncovalent interactions could be identified as spike regions with low electron density and low reduced gradient[24].

To further discriminate different types of noncovalent interactions (such as hydrogen bonding, van der Waals force, and steric crowding), the sign of the Laplacian of the density, sign(λ_2) ρ, is used. A large and negative sign(λ_2) ρ indicates attractive interactions (*e.g.*, dipole-dipole and hydrogen bonding), a large and positive sign(λ_2) ρ suggests nonbonding interaction (e.g., steric crowding), whereas van der Waals force normally manifests itself as a small negative sign(λ_2) ρ value near zero[24]. Therefore, in polyesters, only weak van der Waals force (green spike with sign(λ_2) ρ = –0.008 a.u. in Fig. 2d) and steric crowding (brown spike with sign(λ_2) ρ = 0.007 a.u. in Fig. 2d) exist between the neighboring repeating units, while in polyamides, besides van der Waals force and steric crowding, hydrogen bonding also appears, as indicated by the blue spike with a large negative sign(λ_2) ρ of –0.026 a.u. (Fig. 2f).

The gradient isosurfaces shown in Fig. 2c and 2e, being colored according to the corresponding values of sign(λ_2) ρ, provide a direct visualization of noncovalent interactions in A3 and B3 as broad regions of real space, respectively. In Fig. 2c, interactions between neighboring ester groups only contain van der Waals force and steric crowding, as indicated by the green and brown isosurfaces pointed out by a black arrow in the enlarged image. In Fig. 2e, not only van der Waals force and steric crowding but also strong hydrogen bonding (light blue isosurface pointed out by a black arrow in the enlarged image) dominate the interactions between amide groups in B3. These observations are well consistent with the results shown in Fig. 2d and 2e. The s versus ρ plots of A1, A2, B1 and B2 from NCI analysis are shown in Fig. S6, and the corresponding sign(λ_2) ρ values of different noncovalent interactions of these polymers are detailed in supporting information. The binding energy of hydrogen bonding could be estimated according to an equation developed by Saeedreza Emamian, $\Delta E \approx -223.08 \times \rho(r_{BCP}) + 0.7423$. After filling the $\rho(r_{BCP})$ of B1, B2 and B3 into the equation, the binding energies of hydrogen bonding of B1, B2 and B3 are calculated to be –4.94, –5.08 and –4.92 kcal/mol, respectively[27].

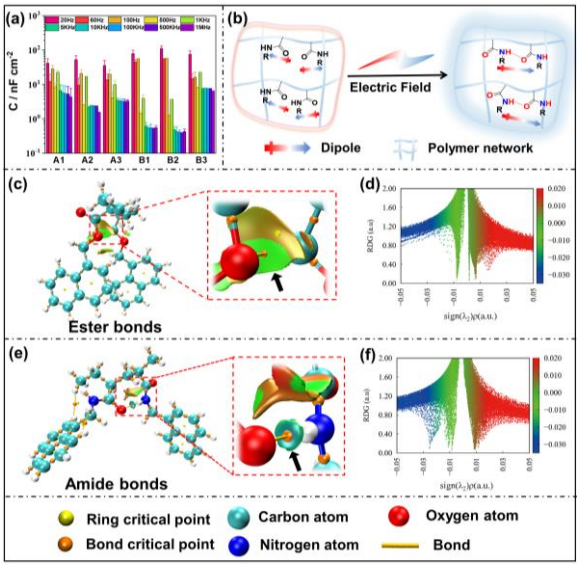

Fig. 2. (a) Capacitance versus frequency plots of six polymers. (b) Proposed mechanisms for the higher capacitance of polyamides. (c) NCI analysis of polyesters (A1, A2 and A3) and (d) plot of reduced density gradient (RDG) versus sign(λ_2) ρ of A3. (e) NCI analysis of polyamides (B1, B2 and B3) and (d) plot of RDG versus sign(λ_2) ρ of B3

The leakage current density of the polymers is shown in Fig. S7. All these polymers show reasonably low leakage current ranging from 10^{-10} to 10^{-6} A/cm^2 at thickness of 1000 nm, depending on the voltage applied. Generally, polyesters exhibit better resistance to leakage, while polyamides are more leaky, probably due to the higher hydrophilicity of

polyamides. Increasing the rigidity of the pendant group again shows negligible impact to the leakage current density (Fig. S7).

After characterizing the polymer dielectrics, we next evaluate their performances in OTFTs with a typical bottom-gate top-contact device architecture (Fig. 1c). To maintain the integrity of the polymer dielectric layer, thermally evaporated pentacene is employed as a semiconducting layer, rather than spin-coated polymer semiconductor from solutions (such as P3HT in toluene). Gold is used as source and drain electrode. As would be expected, all these OTFTs give a typical *p*-type switching behavior (Fig. 3 and Fig. S8) with their mobilities ranging from 2.2×10^{-2} to 6.1×10^{-1} $cm^2V^{-1}s^{-1}$, on/off ratio spanning from 10^2 to 10^5, and V_{th} across from –30 to –55 V. All these data are summarized in Table 1. Interestingly, though the capacitance of polyamides is twice the capacitance of polyesters, the saturated I_d at V_g = –75 V is not significantly different when comparing polyamide OTFTs and the corresponding polyester OTFTs, probably due to the higher mobility of polyester OTFTs. It is known that a hydrophobic dielectric surface is good for charge transport due to a lower density of charge trapping sites, and vice versa. The trap density on dielectric surfaces could be calculated by equation: $N_{tr} = C_tV_{th}/Q$, where N_{tr} is the trap density, C_t is the capacitance of polymer dielectrics and Q is the elementary charge[28]. Table 1 shows the calculated N_{tr} of six polymers are ranging from 9.3×10^{12} to 3.1×10^{13} cm^{-2}, similar to the previously reported values of polymer dielectrics[28]. In addition, polyamides give higher N_{tr} than polyesters, well consistent with the fact that more hydrophilic amide groups could serve as charge carrier traps. The higher charge trap density in polyamide could also well-suppress the residual current in the channel, thus leading to low I_{off} and higher on/off ratios than polyester OTFTs (Table 1).

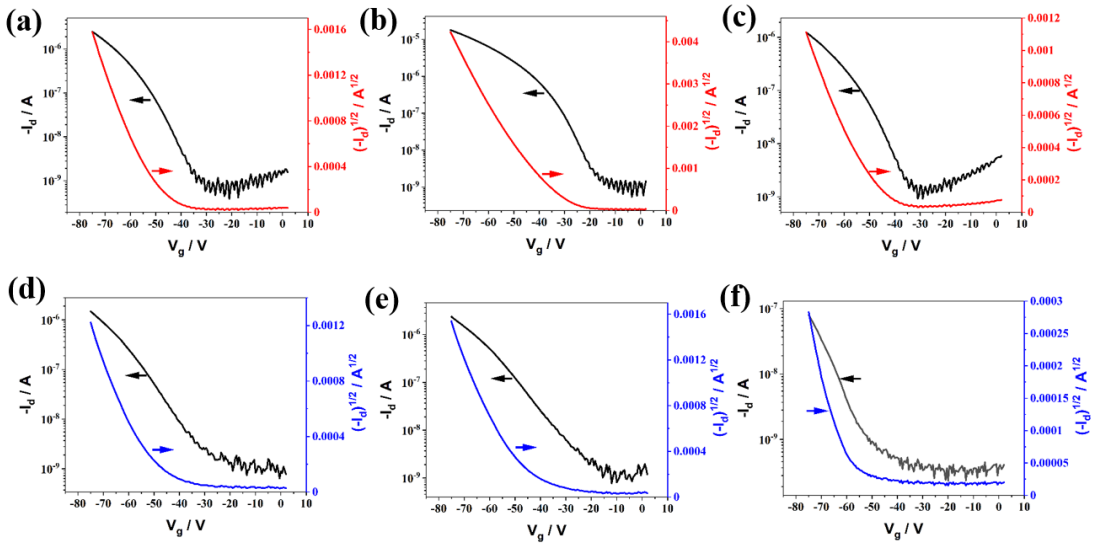

Fig. 3. Transfer curves of OTFTs with (a-c) A1-A3 and (d-f) B1-B3 as dielectric layer

Table 1. Summarization of Capacitance, Molecular Weight, Mobility, on/off Ratio, Threshold Voltage and Charge Trap Densities of Six Polymer Dielectrics

Sample	Capacitance @20Hz(nF/cm^{-2})	K @20Hz	μ_{FET} ($cm^2V^{-1}s^{-1}$)	I_{on}/I_{off}	V_{th} (V)	N_{tr} (cm^{-2})
A1	41.5±14.6	2.4	$(4.7\pm1.6)\times10^{-1}$	$> 10^4$	–45±8.5	1.2×10^{13}
A2	52.4±16.7	3.1	$(6.1\pm2.6)\times10^{-1}$	$\sim 10^5$	–30±5.5	9.8×10^{12}
A3	35.3±14.1	2.1	$(3.2\pm0.2)\times10^{-1}$	$> 10^3$	–42.5±7	9.3×10^{12}
B1	79.4±18.2	4.6	$(1.8\pm0.4)\times10^{-1}$	$\sim 10^3$	–48±11	2.4×10^{13}
B2	111.4±21.3	6.5	$(1.7\pm0.5)\times10^{-1}$	$\sim 10^3$	–45±6	3.1×10^{13}
B3	75.6±20.4	4.4	$(2.2\pm0.4)\times10^{-2}$	$> 10^2$	–55±12	2.6×10^{13}

Notably, dual sweeping of the OTFT transfer curves (V_d = –75 V, V_g sweeps from 2 V to –75 V then back to 2 V) reveal significant differences in the hysteresis behavior of six polymer dielectrics[29]. As shown in Fig. 4, polyester OTFTs generally show well-overlapped transfer curves at forward and reverse sweeping directions except A3, which gives rise to small but detectable hysteresis behavior. In contrast, all polyamide OTFTs show relatively larger hysteresis loops, indicating poor bias-stress stability[30]. To quantify their hysteresis behaviors, we tentatively define the hysteresis ratio as the ratio of the hysteresis loop area to the total sweeping area (I_{max} * (V_{stop} – V_{start})). As shown, OTFT with A1, A2 and A3 dielectric layer gives 9.4‰, 3.8‰ and 2.6% hysteresis ratio, respectively, while that with B1, B2 and B3 dielectric layer shows 6.3%, 6.8% and 8.3% hysteresis ratio, respectively, which are about 3 to 18 times higher than OTFT with corresponding polyester dielectric layer, indicating that the hydrophilic amide could induce large hysteresis probably due to its better charge trapping ability. Further, increasing the π electron delocalization of the pendant groups generally enhances the hysteresis ratio. Particularly for the naphthalene group, a remarkable increment (1.3 to 6.6 times) of hysteresis ratio is observed.

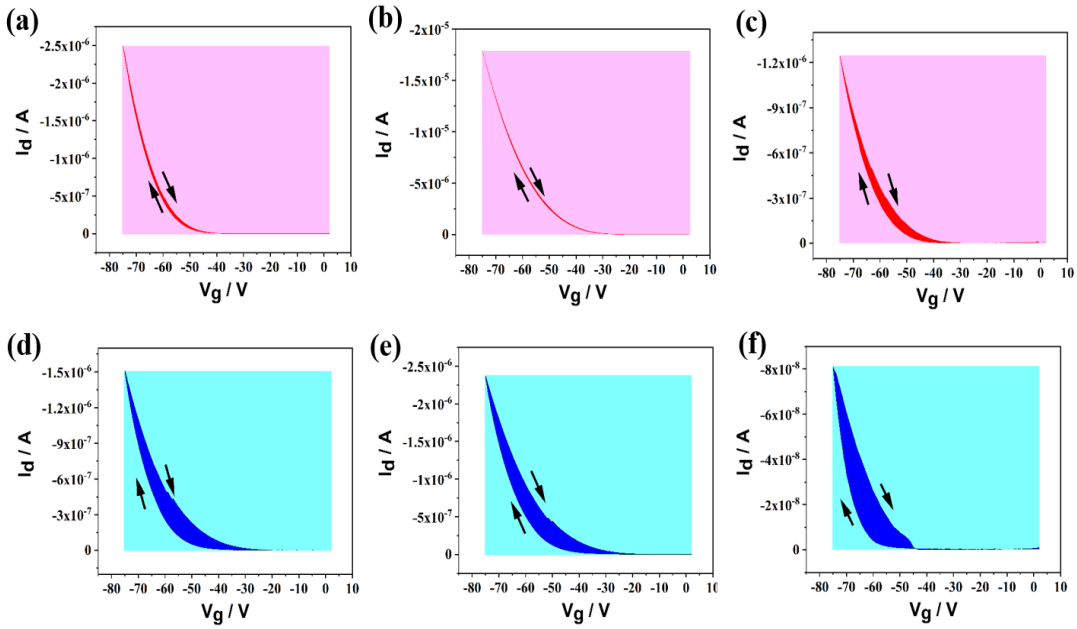

Fig. 4. Hysteresis behavior of OTFTs with (a) A1, (b) A2, (c) A3, (d) B1, (e) B2 and (f) B3 as dielectrics. The arrows indicate the loops' direction. The number in each figure represents the memory ratio of corresponding OTFT

To provide more insights into the hysteresis behavior of these OTFTs with different polymer dielectrics, we next investigate the charge injection barriers between pentacene and different polymer dielectrics. As known (Fig. 5), one major mechanism of the hysteresis behavior is the trapping of charge carriers in the dielectric layer. In this case, the efficiency or the energy barrier of hole injection from pentacene to polymer dielectric layer plays a decisive role in determining the hysteresis behavior of OTFTs. Therefore, the gap between the LUMO of pentacene and polymer dielectric layer is a criterion to assess the hole injection efficiency. Though the exact HOMO and LUMO levels of the polymers are difficult to measure, the monomer energy level of each corresponding polymer could be used as an indicator to evaluate the energy gap between the LUMO of pentacene and polymer dielectric layer (Table S2)[20]. Here, the HOMO and LUMO energy levels of these monomers are calculated by Density Functional Theory (DFT) and listed in Table 2 as well as in Fig. 5a. As the π electron delocalization of the pendant groups increases, the bandgap narrows, and the LUMO level increases and approaches to the LUMO of pentacene. As a result, the hole injection barriers reduce, leading to a high hole injection efficiency, and thus more pronounced hysteresis behavior.

Table 2. Summarization of Hysteresis Ratio, Dipole Moment, Hydrogen Binding Energy, Energy Level and Bond Critical Point of Six Polymer Dielectrics and Corresponding Devices

Dielectric	Hysteresis ratio	Dipole moment (monomer)	Hydrogen binding energy (kcal/mol)	Energy level of monomer (eV)		Bcp (a.u.)
				HOMO	LUMO	
A1	9.4‰	2.6	N/A	–7.5	0.25	N/A
A2	3.8‰	2.2	N/A	–6.95	–0.68	N/A
A3	2.6%	2.3	N/A	–6.08	–1.38	N/A
B1	6.3%	3.9	–4.94	–7.15	0.65	0.0255
B2	6.8%	3.8	–5.08	–6.75	–0.69	0.0261
B3	8.3%	3.8	–4.92	–6.04	–1.34	0.0254

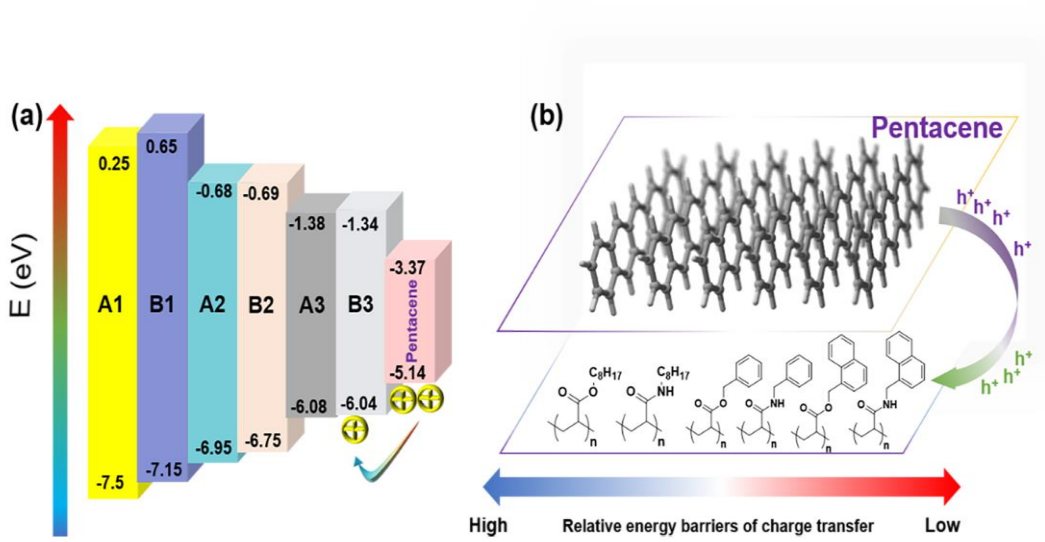

Fig. 5. (a) Energy level of six dielectric polymers related to pentacene. (b) Schematic illustration of relative energy barriers of charge transfer from pentacene to six polymer dielectrics in OTFTs

4 CONCLUSION

In conclusion, we have synthesized a series of well-defined polyesters and polyamides containing pendant groups with progressively enhanced π electron delocalization. NCI analysis indicates strong hydrogen bonding exists between neighboring pendant groups in polyamides, but not in polyesters. In addition, amide groups exhibit much larger dipole moment than ester groups. Attributed to the synergistic effect of hydrogen bonding interaction and higher dipole moment, the polyamide dielectrics exhibit higher κ and surface charge trapping density, and better charge storage capability than the corresponding polyester dielectrics. As a result, OTFTs with polyamide dielectric show lower mobilities, higher on/off ratios, more pronounced hysteresis and higher surface charge trapping densities than the corresponding OTFTs with polyester dielectric. Moreover, as the π electron delocalization increases, the energy barrier between the nearest molecular orbital levels of semiconductor (LUMO) and the polymeric dielectric reduces, which facilitates the hole injection from conductive channel to dielectric layer upon biasing with gate voltages and leads to higher bias-stress instability and larger hysteresis. By combining experimental characterization and theoretical analysis, this work provides a comprehensive study on the distinct properties of different polymer dielectrics, which may help to gain a clearer understanding of the relationship between structures and properties of polymeric dielectrics, and shine light on the design of polymeric dielectrics for OTFTs with different applications.

REFERENCES

(1) Ortiz, R. P.; Facchetti, A.; Marks, T. J. High-k organic, inorganic, and hybrid dielectrics for low-voltage organic field-effect transistors. *Chem. Rev.* **2010**, 110, 205–239.

(2) Wang, B.; Huang, W.; Chi, L.; Al-Hashimi, M.; Marks, T. J.; Facchetti, A. High-k gate dielectrics for emerging flexible and stretchable electronics. *Chem. Rev.* **2018**, 118, 5690–5754.

(3) Magliulo, M.; Manoli, K.; Macchia, E.; Palazzo, G.; Torsi, L. Tailoring functional interlayers in organic field-effect transistor biosensors. *Adv. Mater.* **2015**, 27, 7528–7551.

(4) Lee, W.; Kim, D.; Rivnay, J.; Matsuhisa, N.; Lonjaret, T.; Yokota, T.; Yawo, H.; Sekino, M.; Malliaras, G. G.; Someya, T. Integration of organic electrochemical and field-effect transistors for ultraflexible, high temporal resolution electrophysiology arrays. *Adv. Mater.* **2016**, 28, 9722–9728.

(5) Li, Y.; Huang, X.; Hu, Z.; Jiang, P.; Li, S.; Tanaka, T. Large dielectric constant and high thermal conductivity in poly(vinylidene fluoride)/barium titanate/silicon carbide three-phase nanocomposites. *ACS Appl. Mater. Interfaces* **2011**, 3, 4396–4403.

(6) Byun, H. R.; You, E. A.; Ha, Y. G. Multifunctional hybrid multilayer gate dielectrics with tunable surface energy for ultralow-power organic and amorphous oxide thin-film transistors. *ACS Appl. Mater. Interfaces* **2017**, 9, 7347–7354.

(7) Everaerts, K.; Emery, J. D.; Jariwala, D.; Karmel, H. J.; Sangwan, V. K.; Prabhumirashi, P. L.; Geier, M. L.; McMorrow, J. J.; Bedzyk, M. J.; Facchetti, A.; Hersam, M. C.; Marks, T. J. Ambient-processable high capacitance hafnia-organic self-assembled nanodielectrics. *J. Am. Chem. Soc.* **2013**, 135, 8926–8939.

(8) Wang, Y.; Huang, X.; Li, T.; Li, L.; Guo, X.; Jiang, P. Polymer-based gate dielectrics for organic field-effect transistors. *Chem. Mater.* **2019**, 31, 2212–2240.

(9) Yi, H. T.; Payne, M. M.; Anthony, J. E.; Podzorov, V. Ultra-flexible solution-processed organic field-effect transistors. *Nat. Commun.* **2012**, 3, 1259.

(10) Wu, Y. L.; Lin, J. J.; Ma, C. M. Fabrication of an organic thin-film transistor by direct deposit of a pentacene layer onto a silicon substrate. *J. Phys. Chem. Solids* **2008**, 69, 730–733.

(11) Jang, J.; Nam, S.; Chung, D. S.; Kim, S. H.; Yun, W. M.; Park, C. E. High t_g cyclic olefin copolymer gate dielectrics for N,N′-ditridecyl perylene diimide based field-effect transistors: improving performance and stability with thermal treatment. *Adv. Funct. Mater.* **2010**, 20, 2611–2618.

(12) Nugraha, M. I.; Häusermann, R.; Watanabe, S.; Matsui, H.; Sytnyk, M.; Heiss, W.; Takeya, J.; Loi, M. A. Broadening of distribution of trap states in PbS quantum dot field-effect transistors with high-k dielectrics. *ACS Appl. Mater. Interfaces* **2017**, 9, 4719–4724.

(13) Veres, J.; Ogier, S. D.; Leeming, S. W.; Cupertino, D. C.; Mohialdin Khaffaf, S. Low-k insulators as the choice of dielectrics in organic field-effect transistors. *Adv. Funct. Mater.* **2003**, 13, 199–204.

(14) Xia, Y.; Cho, J. H.; Lee, J.; Ruden, P. P.; Frisbie, C. D. Comparison of the mobility-carrier density relation in polymer and single-crystal organic transistors employing vacuum and liquid gate dielectrics. *Adv. Mater.* **2009**, 21, 2174–2179.

(15) Sun, X.; Liu, Y.; Di, C. A.; Wen, Y.; Guo, Y.; Zhang, L.; Zhao, Y.; Yu, G. Interfacial heterogeneity of surface energy in organic field-effect transistors. *Adv. Mater.* **2011**, 23, 1009–1014.

(16) Kim, C.; Facchetti, A.; Marks, T. J. Polymer gate dielectric surface viscoelasticity modulates pentacene transistor performance. *Science* **2007**, 318, 76–80.

(17) Orgiu, E.; Locci, S.; Fraboni, B.; Scavetta, E.; Lugli, P.; Bonfiglio, A. Analysis of the hysteresis in organic thin-film transistors with polymeric gate dielectric. *Org. Electron.* **2011**, 12, 477–485.

(18) Yang, H.; Kim, S. H.; Yang, L.; Yang, S. Y.; Park, C. E. Pentacene nanostructures on surface-hydrophobicity-controlled polymer/SiO_2 bilayer gate-dielectrics. *Adv. Mater.* **2007**, 19, 2868–2872.

(19) Alameddine, B.; Rice, A. H.; Luscombe, C.; Jenny, T. A. Synthesis of arylamine tribenzopentaphenes and investigation of their hole mobility. *ChemistryOpen* **2015**, 4, 453–456.

(20) Baeg, K. J.; Noh, Y. Y.; Ghim, J.; Lim, B.; Kim, D. Y. Polarity effects of polymer gate electrets on non-volatile organic field-effect transistor memory. *Adv. Funct. Mater.* **2008**, 18, 3678–3685.

(21) Kumar, R.; Goswami, M.; Sumpter, B. G.; Novikov, V. N.; Sokolov, A. P. Effects of backbone rigidity on the local structure and dynamics in polymer melts and glasses. *Phys. Chem. Chem. Phys.* **2013**, 15, 4604–4609.

(22) Zhang, H. C.; Deng, R. N.; Wang, J.; Li, X.; Chen, Y. M.; Liu, K. W.; Taubert, C.; Cheng, S. Z. D.; Zhu, Y. Crystalline organic pigment-based field-effect transistors. *ACS Appl. Mater. Interfaces* **2017**, 9, 21891–21899.

(23) Zhang, H. C.; Li, R.; Deng, Z. F.; Cui, S. W.; Wang, Y. H.; Zheng, M.; Yang, W. J. π-Conjugated oligomers based on aminobenzodifuranone and diketopyrrolopyrrole. *Dyes Pigm.* **2020**, 181, 108552.

(24) Johnson, E. R.; Keinan, S.; Mori-Sánchez, P.; Contreras-García, J.; Cohen, A. J.; Yang, W. Revealing noncovalent interactions. *J. Am. Chem. Soc.* **2010**, 132, 6498–6506.

(25) Wu, P.; Chaudret, R.; Hu, X.; Yang, W. Noncovalent interaction analysis in fluctuating environments. *J. Chem. Theory. Comput.* **2013**, 9, 2226–2234.

(26) Contreras-García, J.; Yang, W.; Johnson, E. R. Analysis of hydrogen-bond interaction potentials from the electron density: integration of noncovalent interaction regions. *J. Phys. Chem. A* **2011**, 115, 12983–12990.

(27) Emamian, S.; Lu, T.; Kruse, H.; Emamian, H. Exploring nature and predicting strength of hydrogen bonds: a correlation analysis between atoms-in-molecules descriptors, binding energies, and energy components of symmetry-adapted perturbation theory. *J. Comput. Chem.* **2019**, 40, 2868–2881.

(28) Ji, D.; Li, T.; Liu, J.; Amirjalayer, S.; Zhong, M.; Zhang, Z. Y.; Huang, X.; Wei, Z.; Dong, H.; Hu, W.; Fuchs, H. Band-like transport in small-molecule thin films toward high mobility and ultrahigh detectivity phototransistor arrays. *Nat. Commun.* **2019**, 10, 12.

(29) Wu, X.; Feng, S.; Shen, J.; Huang, W.; Li, C.; Li, C.; Sui, Y.; Huang, W. Nonvolatile transistor memory based on a high-k dielectric polymer blend for multilevel data storage, encryption, and protection. *Chem. Mater.* **2020**, 32, 3641–3650.

(30) Tsai, T. D.; Chang, J. W.; Wen, T. C.; Guo, T. F. Manipulating the hysteresis in poly(vinyl alcohol)-dielectric organic field-effect transistors toward memory elements. *Adv. Funct. Mater.* **2013**, 23, 4206–4214.

(31) Weigend, F.; Ahlrichs, R. Balanced basis sets of split valence, triple zeta valence and quadruple zeta valence quality for H to Rn: design and assessment of accuracy. *Phys. Chem. Chem. Phys.* **2005**, 7, 3297–3305.